Modeling EDFA Gain Ripple and Filter Penalties with Machine Learning for Accurate QoT Estimation

Ankush Mahajan, Konstantinos Christodoulopoulos, Ricardo Martínez, *Senior Member, IEEE*, Salvatore Spadaro, *Senior Member, IEEE*, and Raül Muñoz, *Senior Member, IEEE*

Abstract— **For reliable and efficient network planning and operation, accurate estimation of Quality of Transmission (QoT) before establishing or reconfiguring the connection is necessary. In optical networks, a design margin is generally included in a QoT estimation tool (Qtool) to account for modeling and parameter inaccuracies, ensuring the acceptable performance. In this work, we use monitoring information from an operating network combined with supervised machine learning (ML) techniques to understand the network conditions. In particular, we model the penalties generated due to *i.)* Erbium Doped Fiber Amplifier (EDFA) gain ripple effect, and *ii.)* filter spectral shape uncertainties at Reconfigurable Optical Add and Drop Multiplexer (ROADM) nodes. Enhancing the Qtool with the proposed ML regression models yields estimates for new or reconfigured connections that account for these two effects, resulting in more accurate QoT estimation and a reduced design margin. We initially propose two supervised ML regression models, implemented with Support Vector Machine Regression (SVMR), to estimate the individual penalties of the two effects and then a combined model. On Deutsche Telekom (DT) network topology with 12 nodes and 40 bidirectional links, we achieve a design margin reduction of ~1dB for new connection requests.**

Index Terms— **Erbium Doped Fiber Amplifier (EDFA), Filter cascading, Machine Learning, network margins, parameter uncertainties, Quality of Transmission (QoT)**

I. INTRODUCTION

THE rapid development of emerging services and applications such as cloud computing, high-definition video streaming etc. along with the latest networking paradigms (e.g., Internet of Things) require higher capacity and QoT guaranteed end-to-end performance [1], [2]. Emerging Elastic Optical Networks (EONs) have introduced flexibility in the optical transport, supporting heterogeneous data rates, optical spectrum channels, modulation formats, etc. [3], [4]. This leads to higher spectral efficiency and capacity, while keeping the network costs as low as possible [1], [5]. For effective optical network planning, it is necessary to estimate the QoT of the connections prior to their establishment. This requires accurate models or tools to estimate the QoT of new or reconfigured connections. However, although EONs provide vast optimization dimensions, optical networks are traditionally planned to be operated statically. In such static network operating mode, high margins are included in the planning phase to ensure acceptable QoT performance up to the end of life [6], [7]. Lowering the margins and increasing efficiency reduces the network cost, motivating various research directions.

Typically, QoT estimation is performed using an analytical Physical Layer Model (PLM) [8] which is included in the QoT estimation tool or Qtool. ML-based estimation techniques are gaining a lot of attention to improve Qtool accuracy [9]-[11]. The main sources of noise accounted in Qtools are the Amplified Spontaneous Emission (ASE) noise generated at both span and node amplifiers and the Non-Linear Interference (NLI) noise, which considers fiber non linearities, mostly self- and cross-channel interferences (i.e., SCI and XCI). A common practice is to add a design margin to the Qtool to account for the modelling simplification assumptions and other uncertainty parameters [6]. Removing such uncertainties would allow the increase of estimation accuracy and an equivalent reduction in the margins, leading to higher efficiency and/or lower cost during network planning and upgrading.

EDFAs [12] are key devices in wavelength division multiplexed (WDM) and EON transport networks that ensure the required connection QoT level at the receivers [13]. However, EDFAs are the dominant noise source (amplified spontaneous emission -ASE noise) in those networks [14]. Typically, span EDFAs are operated in Automatic Gain Control (AGC) mode with near to zero tilt (first order/ linear correction) to get a relatively flat gain in the C-band [15]. Although the gain tilt is maintained at zero there are still fluctuations/ripples within the gain bandwidth of EDFAs. These gain ripples may be due to: i) residual imperfections in the gain flattening filters;

Ankush Mahajan (e-mail: ankush.mahajan@cttc.cat), Ricardo Martínez (e-mail: ricardo.martinez@cttc.cat) and Raül Muñoz (e-mail: raul.munoz@cttc.cat) are with Centre Tecnològic de Telecomunicacions de Catalunya, CTTC/CERCA, Castelldefels, 08860, Spain.

Konstantinos Christodoulopoulos is with Nokia Bell Labs, Stuttgart, 70435, Germany (e-mail: konstantinos.1.christodoulopoulos@nokia-bell-labs.com).

Salvatore Spadaro is with the Dept. of Signal Theory and Communications, Universitat Politècnica de Catalunya, UPC, Barcelona, 08034, Spain (e- mail: spadaro@tsc.upc.edu).

and or ii) wavelength dependent absorption/ emission coefficients of Er^{3+} ions [16], [17]. Also, typically, PLMs / Qtools assume that the EDFAs have constant noise figure (NF) across all WDM channels. Although NF mainly depends on the population inversion of erbium ions and follows McCumber theory [18], small NF variations across transmission band are expected.
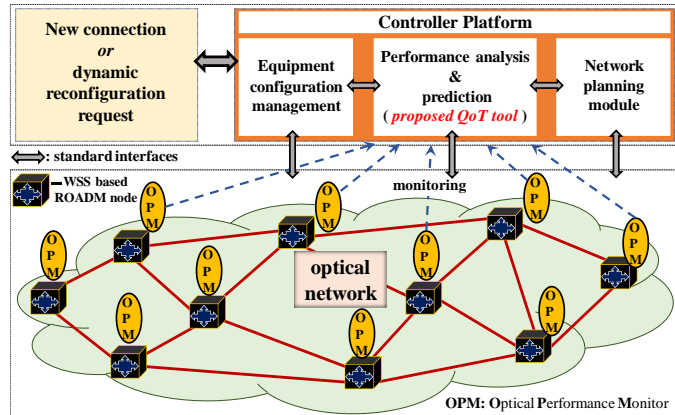

Fig. 1. An example of EON indicating OPMs installed at each node and location of the proposed ML assisted Qtool

ROADMs based on wavelength selective switches (WSSs) is another key element in WDM or EONs. ROADMs support the colorless and/or directionless and/or contention less (CDC) multiplexing and demultiplexing at the network nodes [19]-[21]. However, the WSS of the ROADMs are essentially strong filters. They narrow the signal bandwidth (BW), a problem which becomes severer as the number of WSSs/ROADMs are cascaded over long paths [22], [23]. Consequently, this causes optical filtering penalty that needs also to be modeled precisely and/or covered in the pre-allocated margins. Authors in [23] investigated the ROADM node penalty. Their studies found that filtering penalty increases exponentially as the number of traversed nodes increases, as well as that the penalty varies with respect to the modulation format and frequency grid spacing. In a deployed network, there are uncertainties in such penalties; slight variations in filters spectral responses are typical even for identical filters, while the transmitter laser and the filter central wavelengths could be misaligned. These uncertainties grow even higher for heterogeneous nodes with different types of filters (e.g., in multi-vendor scenarios [24]-[26]). In light of the above, it is quite challenging to estimate the corresponding accumulated penalties.

Several recent studies and also optical equipment vendors are considering the installation of optical performance monitors (OPMs) at nodes to support enhanced network operations [27]. Using OPMs we can extract information and train ML (supervised) models for better understanding of the actual physical condition. In our previous work [28], with the help of electrical SNR monitors at each node, we accurately estimated the gain ripple penalties for new connections requests. Extending our previous work, in this paper, we only use optical data (OPMs) at intermediate nodes and electrical SNR monitoring at the coherent receivers. To be more specific, we propose a Qtool that uses optical monitored information of

established connections to train supervised ML regression models, implemented using SVMR, for better prediction of QoT for the new connection requests. The proposed ML assisted Qtool provides the performance prediction module at the network controller and is trained by using OPMs and receivers information (Fig. 1) [29]. When the network is upgraded (e.g., by adding one or a batch of new connections) or when new connections are dynamically established or reconfigured, the use of the trained ML Qtool allows for lower margins.

The reminder of this paper is organized as follows. In Sections II we overview the related work. Then in Section III we report on baseline experiments and simulations that expose the effects of gain ripple and filtering uncertainties. In Section IV, we present the mathematical modelling for the two effects, independently and then jointly. Next, in Section V, we detail the proposed ML based Qtool, highlighting the modelling and feature extraction steps. Then in Section VI, we show the performance evaluation of the proposed solutions, followed by related discussions. Finally, Section VII concludes the paper.

II. RELATED WORK

There are several factors which impact the accuracy of the Qtools and cause estimation uncertainty. To embrace such uncertainty in the Qtool estimation, design margins are used. Qtools range from analytical models to more advanced ML-estimation techniques that make use of monitored information. All the approaches presented in [8]-[10] assume a flat EDFA gain. This requires high design margins to address the QoT estimation inaccuracy (e.g., 2-3dB in SNR [6], [7]). In addition to this, Qtools assume either constant or more realistic exponential OSNR penalty as the number of cascaded ROADM nodes grows [22]. Indeed, works in [22], [23] verified that this exponential function depends upon both the modulation format and the frequency grid spacing. All these prior works did not consider the uncertainty due to small fluctuations in filter's spectral response/shape and its effect on the accuracy of the Qtool. This problem can exacerbate if we follow the latest trend of disaggregated optical architectures, where ROADM nodes or even WSS components come from different vendors. Indeed, the cascading effects of such multi-vendor ROADMs would be more severe when compared to traditional aggregated optical network scenarios.

A. Related Work: EDFA Gain Ripple

The OSNR is a function of the traversed spans and particularly depends upon the gain ripple profile of each span EDFA [17]. The authors in [14], [26] presented the effects of gain ripples on span EDFAs, leading to uncertain OSNR estimation. They also explored the effects of variation in the operating conditions of span EDFAs (monitored by tapping the signal at each span EDFA) to minimize the OSNR penalty due to gain ripple. The authors in [30], [31] proposed a pre-emphasis launch power technique to reduce the EDFA gain ripple effects. This technique is well suited for fully loaded links and requires precise control at the transmitter. The work in [31] use approximate analytical models to calculate noise at

full channel loading conditions. However [31] verified once more that EDFA gain ripple affects the quality of signal, hence SNR. A gradient descent-based launch power optimization strategy was used to improved SNR in this work. However, all the span EDFAs gain ripple profiles were assumed to be identical, which, in general, is not realistic in deployed networks. Apart from these attempts, several analytical models were also proposed to estimate EDFA wavelength dependent gain and channel output power, under different channel loading conditions. In general, all these models range from limited accuracy and simple characterization to very detailed estimations, trading-off processing time for accuracy. In [32] authors proposed an accurate ML model with cascaded EDFAs as a first step toward channel assignment/ resource allocation. However, the benefits in terms of accuracy improvement or margin reduction for QoT estimation were not presented. A most recent extension of EDFA gain spectrum modelling (in [33]) based on a hybrid (analytical and experimental dataset based neural network ML model) approach was presented in [34]. Some other recent ML-based works addressed the wavelength dependent gain spectra estimation [31], [35]. In [36], [37] neural network models were also proposed to recommend wavelength assignment with 99% of precision value that considers EDFA gain ripple effects. In [35] a single EDFA modelling required 18000 channel loading conditions. The cascade of EDFAs and its effect on gain ripples were also not considered. The dataset used for training those models were either i) analytical without considering fiber effects/NLI noise contribution, or ii) experimental which needs the data collection of each individual span EDFA. These requirements practically constrain the usability of those approaches. In [14], the gain uncertainties of EDFA working in AGC mode was experimentally investigated. A method was derived aiming at reducing these gain uncertainties up to 0.5 to 0.7dB when encompassing up to five cascaded EDFA spans. The targeted scenario in [14] was dynamic with the add/drop of new/existing connections. However, for fixed load EDFAs, with static network conditions, the gain ripples effect was not explored. Moreover, optical attenuators were used to replace fibers in the conducted experiments. Hence the effects of NLI noise contribution was not considered at all.

B. Related Work: ROADM Uncertainties

ROADMs consist of WSS filters and amplifiers to route and boost the signal towards the destination node. Generally, a signal that traverses a ROADM suffers from filtering penalty and QoT degradation, as discussed in Section I. Research works in [22], [23] confirmed that ROADM node penalty (in OSNR) increases exponentially with the number of nodes. [38] presented an analytical model based on a higher order SNR-OSNR relation to capture cascaded filtering effects . All these works focused on characterization of the cascade (either by looping single filter, or by replacing cascaded filters with a tunable BW filter) and not on the identification of the quality of the individual filters. [39] proposed an approach for real time cascaded filtering penalty assessment (for different order gaussian filters) and verified it for a commercial 200G 16-

quadrature amplitude modulation (16-QAM) transponder and WSS modules. [39] showed the effect of spectral shape variation in a cascade of filters which resulted in uncertain (as outliers in Fig. 4) OSNR penalty estimation. However, in that work also, the spectral shape variations and corresponding uncertain OSNR penalty estimation were not accounted for. As already discussed, this non-linear penalty is expected to exacerbate in disaggregated optical networks where ROADM/filters and Tx. lasers could come from multiple vendors with diverse characteristics. A recent study on disaggregation at node level indicated 3.5-5dB (core) and 3-3.5dB (metro) required margins [40], mainly due to uncertainties/variability of the multi-vendor components; the filtering penalty of ROADM nodes play a significant part in those increased margins.

In brief, to the best of our knowledge, the effects of EDFA gain ripple and of ROADM filter spectral uncertainty on QoT estimation needs further exploration. The understanding of these two effects could improve QoT estimation accuracy and reduce margin for reconfigured or future connection establishments. Therefore, we devise estimation tools that can predict the independent or combined penalties of the aforementioned effects based on training from monitored data of established connections and achieve a considerable reduction in the required margins.

III. PRELIMINARY STUDIES AND MOTIVATION

The gain profile of the EDFA is not complete flat and suffers from the gain tilt and the gain ripple problems. The former is easily equalized with a first order/linear correction. Hence, we will discuss the compensation of the gain tilt in this paragraph, so as to avoid confusion with the gain ripple in the rest of the paper. In general, an EDFA amplifier card has a flat linear approximated output (gain ripples exist but are higher order terms), i.e. *zero gain tilt*, only for a specific gain value $g_{des.}$, as shown in Fig. 2(a). This value is based on the internal design and is specified by the amplifier manufacturer. If the amplifier operating gain point g_o is not equal to g_{des}, then the output suffers from a gain tilt as shown in Fig. 2(b). This tilt can be compensated at the amplifier card level with well-known methods [15]. A variable optical attenuator (VOA) inside the amplifier is automatically adjusted to obtain the zero-tilt profile (but with gain ripples) at the output (Fig. 2(c)). From now onwards, whenever we will consider the gain ripple of an EDFA, we will assume that the gain tilt is compensated to zero by internally readjusting its operating point to $g_{o} = g_{des}$.

A. Motivation: EDFA Gain Ripple

As discussed above, typically all span EDFAs are operated in AGC mode with near to zero gain tilt, that is flat first order approximated gain in the C-band, as presented in Fig 2(c) and also in Fig. 1 of [14]. To motivate our work and understand the trends of EDFA gain ripple profiles, we performed lab experiments. We used 4 different EDFAs in the optical spectrum band of ~1530 – 1563nm with 40 WDM channels at 100GHz spacing with central frequencies adjusted according to ITU standards as shown in Fig. 3(a). We operated all EDFAs in
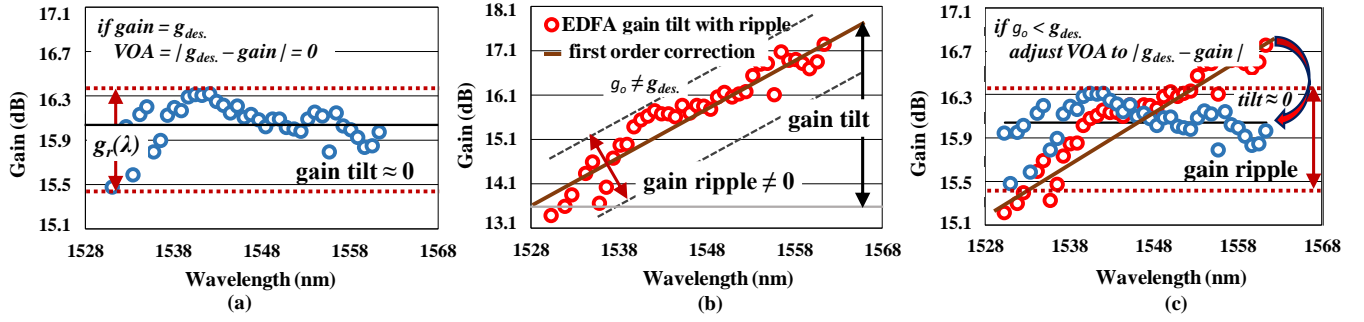
Fig. 2. End to end EDFA gain tilt equalization on experimentally collected (a) ripple profile with gain = $g_{des.}$, VOA = 0dB, (b) $g_o \neq g_{des.}$ leading to gain tilt, (c) first order correction by setting VOA = $|g_{des.} - g_o|$
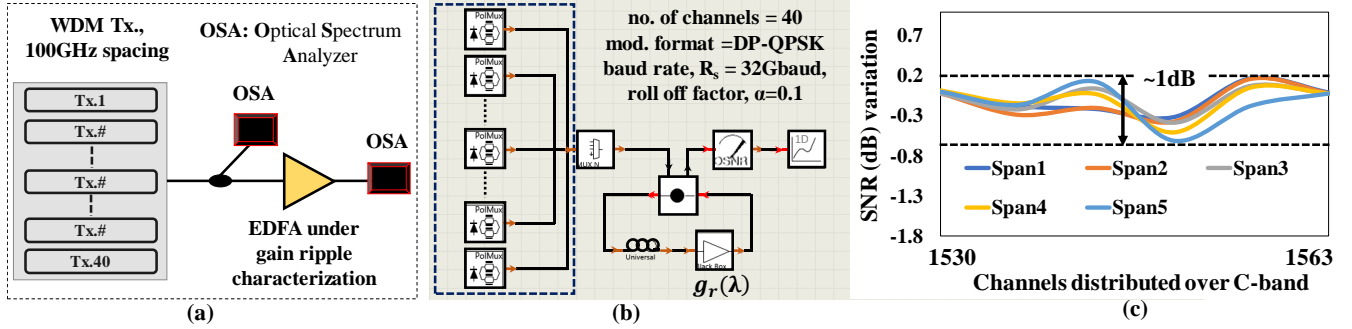

Fig. 3. (a) experimental setup to capture EDFA gain ripple profiles, (b) VPI Tx. Maker set up of 40, 100G DP-QPSK WDM channels having span EDFA gain ripple profile, (c) SNR penalty for ripple of 0.5dB for central channel

AGC mode and zero tilt by pre-adjusting their operating points. The experimental setup used is shown in Fig. 3(a). Based on collected experimental data, we created realistic span EDFA gain profiles denoted by $g_r(\lambda)$, with maximum peak-to-peak value of ±0.5dB (λ denotes the wavelength in C-band, r denotes the 4 characterized EDFAs). We then simulated in VPI Transmission Maker a link with increasing number of spans, each of 80 km and chose one of the experimentally collected $g_r(\lambda)$ profile per simulation. On this link we simulated the transmission of 100GHz spaced 40 Dual Polarization-Quadrature Phase Shift Keying (DP-QPSK) WDM channels as shown in Fig. 3(b). We found ~1dB of fluctuation for the channels after 5 spans (maximum EDFA peak-to-peak ripple of ±0.5dB in all spans) as shown in Fig. 3(c). In general, the shape of the ripple can vary over longer time (aging), but this is a slow process. So, in short and medium term the ripple function has a clear trend which makes its modelling possible. The observed SNR variation upto 1dB due to the gain ripple for only five cascaded spans (Fig. 3(b)) - similar findings are reported in Fig. 7 of [26]- indicate that if the gain ripple is not modelled in the QoT estimator, an equivalent margin (1dB) should be used to cover it.

B. Motivation: Filter Spectral Uncertainties inside ROADM

In current optical networks, connections are generally filtered and routed through multiple ROADM nodes before finally detected at their receivers. We denote a connection c with central wavelength, λ_c and traversed path p_c. We also denote by $F_m(p_c, \lambda_c)$ the spectral response of the filter located at the end of mth link along p_c (ROADM nodes might implement more than one filter but we now focus on just one per link). In general, $F_m(p_c, \lambda_c)$ is characterized by its central frequency, pass-band bandwidth (BW), shape (gaussian, trapezoidal etc.) and order. The central frequency of the filter is defined according to the connection's central wavelength λ_c and its BW is always higher than the connection's BW and according to ITU grid. The filter shape and order depend on the filter type and current generation ROADMs use 2nd order Gaussian shaped filters. Fig. 4(b) shows the spectral shape of the transmitted signal modulated at 32Gbaud and 0.1 roll off factor with DP-QPSK modulation format (blue line) obtained with simulations in VPI Transmission Maker (Fig. 4(a)). As the transmitted signal traverses the nodes/filters, its signal quality is degraded, according to the cascade of the filters' spectral responses, what is known as the filter cascading effect. Fig. 4(b) also shows the spectral shape of the received signal after one, three and five identical cascaded filters (the spectral response F_m was the identical for all $m = 1…,5$). Fig. 4(b) clearly shows that the signal quality degrades as the cascade increases, even for identical filters. In Fig. 4(b), we observed a 3dB BW degradation of ~6.02GHz after 5 identical filters (solid green line). However, as already discussed, in real networks slight variations in filters spectral responses are typical even for identical filters, while the transmitter laser and the filter central wavelengths could be misaligned. Such issues result in inaccurate filtering penalty estimation. We simulated an uncertainty of ±10% in 3dB BW of each filter in VPI Transmission Maker for a cascade of five filters. Fig.4(c), shows the resulted signal 3dB BW at different cascade levels. We observed ~2.1GHz uncertainty in the signal 3dB BW (dotted red line) at the end of the cascade/path. This uncertainty
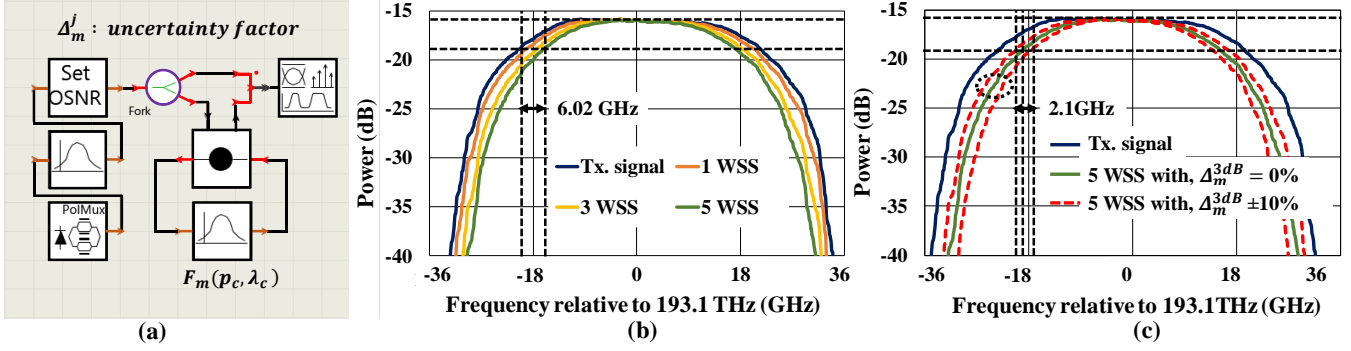
Fig. 4. (a) VPI Tx. Maker set up of single channel, 100G DP-QPSK signal having uncertain filtering, Δ_m at ROADM node, (b) effective 3dB BW reduction after cascading of 5 filter with zero uncertainty $\Delta_m=0$, (c) effective 3dB BW reduction after cascading of identical filter with uncertainty, Δ_m of $\pm 10\%$

would contribute to inaccurate OSNR filter penalty estimation and should be covered by a related margin.

These preliminary results, obtained from the above described experiments and simulations for EDFA gain ripple and spectral uncertainties of filters, motivated us to explore these effects further. Our goal was to integrate them in QoT estimators to yield higher accuracy (or lower design margin) for future connections, as discussed in the upcoming sections.

IV. MATHEMATICAL MODELING OF RIPPLE AND FILTER SPECTRAL UNCERTAINTIES

This section outlines the formulation of EDFA gain ripple and spectral uncertainties of ROADM filters in QoT estimation.

A. Modelling of Ripple Unaware and Aware EDFA Gain

In this subsection, we outline the modelling used in a standard and extended PLM to accounts for the gain ripple. In general, a PLM calculates ASE and NLI noises and adds margins on top for simplifications/ noise contributing factors that it partially covers.

Let us focus on a multi-span link as shown in Fig. 5. Current generation commercial EDFAs are dual staged having low NF, and a large dynamic range (up to 15 dB) [41]. Moreover, in real networks, a Dynamic Gain Equalizer, DGE, is used to compensate the cumulative EFDA gain ripple effect on multi-span links, resulting in almost flat output power [42]. For a typical scenario of a 6 span link the DGE is applied at the 3rd span as shown in Fig. 5. For longer links a new DGE is installed every ~6 spans. Even though the use of DGEs, residual gain ripple effect is still present, affecting the overall QoT estimation accuracy.

The ASE noise (linear noise) estimation is straightforward to model and depends upon the gains and noise-figures of the EDFAs along the path. For NLI several models have been proposed and validated [43]- [46]. The Gaussian Noise (GN) model [44], [46] is computationally very efficient while maintaining good accuracy [26]. Hence, we implemented it and also extended it to account for the additional wavelength dependent gain ripple penalties.

Assume now that we have a connection $c = (p_c, \lambda_c)$ and use the standard GN model that does not model the gain ripple. The SNR at the end of link m on the path p_c calculated with the standard GN model (ripple unaware-RU) is denoted by

$SNR_{RU,m}(p_c, \lambda_c)$, respectively. We can then accumulate the inverse of SNR over the links of the path p_c to obtain the total SNR calculated at connection's end as $SNR_{RU}(p_c, \lambda_c)$. We denote the Qtool that uses the standard GN which is ripple unaware as Q_{RU}. Such tool, since it is ripple unaware, has to use a margin (part of $design\ margin_1$) on top of $SNR_{RU}(p_c, \lambda_c)$ to account for the penalties due to neglected wavelength dependent gain ripples.
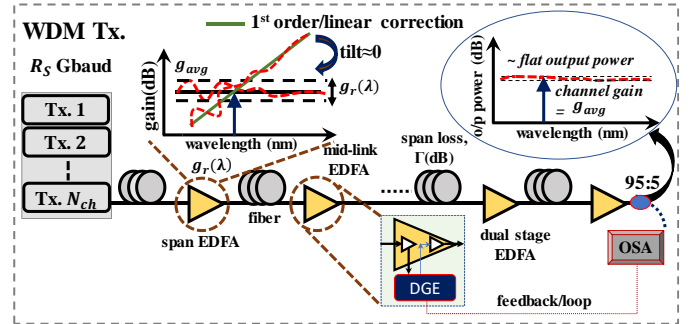

Fig. 5. WDM link indicating span EDFAs with gain ripple, $g_r(\lambda)$ and DGE location with dual stage EDFA resulting in flat output at link end

As discussed, in reality, EDFAs have gain ripples, which makes the power spectral density (PSD) of each channel to change after each traversed span (even for uniform launch power and baudrate). Assuming known ripple profiles $g_{n_s}(\lambda_c)$ of each span n_s we can calculate the PSD of each channel and also the PSD of NLI noise at the end of each span. In deployed networks with DGEs installed at certain spans (as shown in Fig. 5), the DGE alters the power profile of the applied span so as to flatten the output power at the end of the covered spans via a feedback loop. We can account for this in modeling, by setting on the span on which the DGE is applied the signals PSD to be equal to the DGE feedback power profile. This is calculated by the known EDFA ripple profiles so as to obtain zero ripple at the end of the link.

The above described GN model is thus *ripple aware* (RA). We calculate the ASE and NLI noise (including effect of gain ripples) per link, and then, using the per link inverse SNR addition, we obtain the total SNR for connection c, denoted by $SNR_{RA}(p_c, \lambda_c)$. Then, on top of that, we add the *design margin$_2$* to cover for modeling inaccuracies, excluding the gain ripple. We call the Qtool that uses this ripple aware PLM as Q_{RA}. The

details about the assumptions and extensions in the GN model to account for ripple penalties are presented in Appendix1. Note that in case of *ripple aware* Q_{RA} the total noise generated at the end of path is closer to the reality, compared to ripple unaware Q_{RU}, since it models/accounts for the wavelength dependent ripple. This leads to better accuracy and a lower design margin i.e. *design margin$_2$ < design margin$_1$*.

B. Modelling of Filters Spectral Uncertainties inside ROADM

We now discuss briefly the mathematical formulas used for standard and extended PLM to account for the uncertainties in ROADM filtering penalties. As the connection traverses multiple nodes, the OSNR filter penalty accumulates in a nonlinear fashion as shown in Fig. 6 (we used VPI Transmission Maker to measure the penalty for three different modulation formats). We consider the standard CDC *switch & select* (*S&S*) architecture of ROADM node as shown in inset of Fig. 6(a), although our approach can be also used for *broadcast & select* (*B&S*) architecture, or a mix. In S&S, two WSSs are used to route the signal to the outgoing link together with two EDFAs acting as pre and booster amplifier, respectively. For add/drop signal at source/destination node, we assume that the penalty comes from only one WSS/filter. Depending on add/drop or crossing direction, different filters are encountered in the ROADM. To account for this and also for the cascading effect, we account the filters by considering *subpaths*. So, extending the above notation, for connection c that uses path p_c and wavelength λ_c we denote by $p_{c,m}$ the *subpath* from the source/Tx up to link m. We also denote by $S_{p_{c,m}}(p_c, \lambda_c)$ the signal spectrum at the end of link m, due to the cascade of previous filters over the subpath, $p_{c,m}$. This is given by:

$$S_{p_{c,m}}(p_c, \lambda_c) = \prod_{k \in p_{c,m}} F_k(p_c, \lambda_c) \qquad (1)$$

where $F_k(p_c, \lambda_c)$ is the spectral response of filter k in path p_c. In the following, we drop λ_c and p_c for simplicity. From $S_{p_{c,m}}$ we can extract a set of attributes, indexed by j, that reflects the key properties of the cascade up to link m, denoted by $S_{p_{c,m}}^j$. Such attributes can be the 3dB BW, cascaded filter central frequency, signal distribution parameters, etc., or $S_{p_{c,m}}^j = \{S_{p_{c,m}}^{3dB}, S_{p_{c,m}}^{fc}, \dots, S_{p_{c,m}}^{sym.}\}$. However, variations within spectral responses of filters and misalignments result in uncertainties in these attributes $S_{p_{c,m}}^j$ which we denote by $\Delta_{p_{c,m}}^j = \{\Delta_{p_{c,m}}^{3dB}, \Delta_{p_{c,m}}^{fc}, \dots, \Delta_{p_{c,m}}^{sym.}\}$.

Extending this notation to PLM/Qtool, let us consider connection $c=(p_c, \lambda_c)$. The standard PLM would assume that the filters along its path are perfectly identical, $\Delta_{p_{c,m}}^j = 0$. The standard PLM estimates an attribute $s_{p_{c,m}}^j$ (lowercase as opposed to real attributes $S_{p_{c,m}}^j$) at the end of link m, and employs an attribute dependent filter penalty function, w^j, to calculate the attribute at the next link $s_{p_{c,m+1}}^j = w^j(s_{p_{c,m}}^j, F_i)$. An example of such a function for the attribute j=3dB, w^{3dB}, is shown in Fig. 6(a), coming from VPI simulations. We see that the 3dB BW ($s_{p_{c,m}}^{3dB}$) degrades as the function of the cascaded filters. The standard PLM would also employ a function q to

map the attributes $s_{p_{c,m}}^j$ to (modulation format dependent) OSNR penalty at each link end and at the end of the path p_c. An example of such q function that translates 3dB BW to OSNR penalty, according to the channel modulation format is shown in Fig. 6(b), again obtained through VPI. Note that a standard PLM could do the above in one step, go directly from subpaths to filtering penalties, without calculating the attributes, but the above description gives us the intermediate step that helps us model the uncertainties.
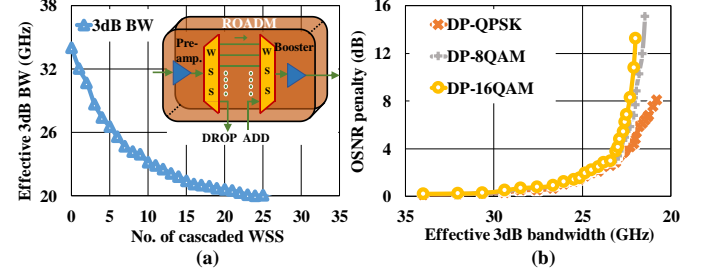

Fig. 6. (a) effective 3dB BW degradation with cascading of WSSs, (b) OSNR penalty function q (in dB) due to tight optical filtering for DP-QPSK, DP-8QAM and DP- 16-QAM as a function of 3dB BW.

We denote the Qtool that uses the filtering uncertainty unaware PLM discussed above by Q_{FU}. This tool calculates the SNR at the end of link m, $SNR_{FU,m}(p_c, \lambda_c)$, and then at the end of the path $SNR_{FU}(p_c, \lambda_c)$, as described in Appendix 2. Since it is filter uncertainty unaware (FU) it has to include in its margin *design margin$_1$* a part to cover the filter penalty uncertainty error. Note that as in the previous section (and also in the next) we denote by *design margin$_1$* the margin of the *unaware* Qtool and by *design margin$_2$* the lower margin of the *aware* Qtool.

However, in real networks there are variations in the spectral responses of filters and misalignments of Tx and filters central channels. For example, as shown in Fig. 4(c), an uncertainty of $\Delta_m^{3dB} \pm 10\%$ in 3dB BW of each filter in a cascade of 5 filters resulted in ~2.1GHz uncertainty in the signal 3dB BW, which according to Fig. 6(b), results in ~0.6 dB in OSNR penalty estimation. Assuming that we know the filtering uncertainties $\Delta_{p_{c,m}}^j$ we can calculate the SNR at the end of each link and at the end of the path $SNR_{FA}(p_c, \lambda_c)$ taking those into account. The details about the assumptions and the extensions to the standard PLM to account for filtering uncertainties are presented in Appendix2. We denote the Qtool that uses this filtering uncertainties aware PLM as Q_{FA}. Such Qtool will use *design margin$_2$* on top of $SNR_{FA}(p_c, \lambda_c)$ to cover other estimation errors, but not of filters. As discussed, it stands to reason that filter uncertainty aware Qtool, Q_{FA}, has a lower design margin i.e. *design margin$_2$ < design margin$_1$*.

C. Combined Mathematical Modelling of EDFA Gain Ripple and Filter Spectral Uncertainties

Lastly, we want to highlight the most realistic case which merges both effects. We consider a standard PLM which assumes EDFA with no ripples and no filtering penalty uncertainties. This PLM/Qtool is a combination of Q_{RU} and Q_{FU}. So, it is *ripple plus filtering uncertainties unaware* (*RFU*) and is denoted by Q_{RFU}. The overall accumulated noise and the

SNR calculated at the end of link m is denoted by $G_{Noise\_RFU,m}(p_c, \lambda_c)$ and $SNR_{RFU,m}(p_c, \lambda_c)$, respectively. We can then calculate the total SNR of the connection as $SNR_{RFU}(p_c, \lambda_c)$, and we add the *design margin₁* to account for inaccurate model of ripple, filters uncertainties, and other factors.

Assuming that we know the gain ripple profiles $g_{n_s}(\lambda_c)$ for all EDFAs and also the uncertainties in the filter responses $\Delta_{p_{c,m}}^j \neq 0$ for all filters. Then we can calculate the PSD of NLI at each link end and the filtering penalty at each node. We combine those to obtain the total SNR at the end of the path p_c, $SNR_{RFA}(p_c, \lambda_c)$. We call this a *ripple and filtering aware* Qtool as Q_{RFA}. Such Q_{RFA} would use *design margin₂* on top of $SNR_{RFA}(p_c, \lambda_c)$ to account for uncertainties other than the two under consideration. The details about the assumptions, extensions and modification in standard PLM to account for both ripple and filtering penalties are presented in detail in Appendix3.

V. MACHINE LEARNING BASED MODELING

In the previous section we outlined the mathematical modeling of the gain ripple and filter response uncertainties. However, such modeling is feasible if we accurately know the gain profiles of the EDFAs $g_{n_s}(\lambda_c)$ and the spectral responses of the filters $F_k(p_c, \lambda_c)$, or their related uncertainties $\Delta_{p_{c,m}}^j$. Such assumptions are rather unrealistic. They would require the measurement of all EDFAs and filters in the network, which would have to be repeated because they would vary with time (aging, traffic changes, etc.). So, in this section we present our proposed solution: use monitoring information in an operating network combined with machine learning (ML) to model the penalties due to these effects. The proposed ML model is trained with the current network state and then used for estimating the 'unseen' penalties of future connections, achieving higher QoT estimation accuracy and requiring lower margins.

We assume an optical network with established connections and their attributes (also referred to as the *state* of network at a given time) denoted by C. Note that C contains the attributes for each connection such as, the traversed path p_c, central wavelength λ_c, transmitted power etc. We also assume that the network has OCMs installed at the end of each link [47], that is, before each ROADM. In Fig. 7, we show a simple network where we indicate the locations of OCMs and main parameters extracted (output power, set of j attributes from monitored spectra $S_{p_{c,m}}^j$ etc.). In Fig. 7, we also indicate the DGEs location that flatten the EDFA gain ripples before every ROADM node, that is, at the end of each link. We also assume that we can monitor the feedback power profiles of the DGEs and also the electrical SNR information at the coherent Rx at the transmission endpoints [27], [28]. Finally, we assume that all monitoring information is made available through a suitable control plane.

We start with a standard Qtool that is gain ripple and/or filtering uncertainty unaware, according to the considered case out of the three described in the previous section (corresponding

unaware tools: Q_{RU}, Q_{FU}, Q_{RFU}). We use the monitored information from established connections to calculate the estimation error of the standard unaware Qtool due to the considered effect. Based on those we train a supervised ML regression model to estimate those errors. The model is then used to calculate the related corrections for new unestablished connections. Then for new connections we use the trained ML model as a correction on the standard unaware Qtool estimation. The main difference of the three considered cases lies in the ML feature extraction and modelling and will be described in the following.
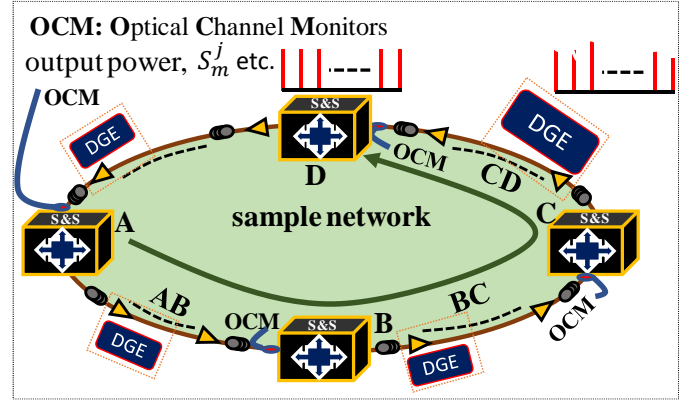

Fig. 7. Sample 4-node network depicting monitoring port locations and DGE placement locations.

A. ML-based gain ripple effect modeling

We assume a ripple unaware PLM Q_{RU}, as discussed in the first half of section IV.A, which calculates the end-to-end noise of each established connection as $G_{Noise\_RU}(p_c, \lambda_c)$, for all connections $c \in C$. As a first step, using the monitored DGE power profiles we can improve such estimations. We use the ripple aware Q_{RA} formulas with flat EDFA gain profiles, but we use the monitored power profiles at the DGE spans. We call this ripple dynamic gain equalizer aware Q_{REA} Qtool. We denote the estimated noise by $G_{Noise\_REA}(p_c, \lambda_c)$ and the set of estimated values for all established connections C by $Y_{REA}(C)$.

We then monitor the electrical SNR of the established connections and thus their noise (ASE and NLI) at the coherent receiver/ path level, $Y_{RA}(C)$ and store it in the Qtool database. This data serves as the ground truth, it defines the true $G_{Noise\_RA}(C)$, with zero margin. We denote the difference of the real/monitored G_{Noise_RA} and the estimated G_{Noise_REA} at path level as $E_R(C) = Y_{REA}(C) - Y_{RA}(C)$. E_R is a vector that includes the estimation errors of Q_{REA} of the established connections due to the real gain ripples. From connections attributes, C, we extract features which depend on connections' routes and central wavelengths. To be more specific, for each connection c we assign its used wavelength on the links that it utilizes (links used in the path are one hot encoded). Additional to these features, a *bias* is also considered to account for any monitoring calibration error and for the non-zero equalized tilt. The per connection features along with the bias term are merged into a *gain ripple features matrix* $X_R = f_{GR}(C)$. The feature matrix enables the correlation between connections crossing the same link while accounting for their utilized wavelengths. Our goal is to identify the function $\Theta_R(X_R) \approx E_R$ that maps well the

features matrix X_R to the penalty E_R generated due to the gain ripple. Based on the monitored information of established connection, we can train supervised ML models on the above features and their corresponding labels, E_R. Under the hood, Θ_R implements a wavelength dependent ripple penalty function per link.

We rely on ML for training and fitting of X_R on E_R and finding the function Θ_R. Assuming a new connection request $r \notin C$, we will use Q_{REA} to obtain the total approximated noise $G_{Noise\_REA} = Y_{REA}(r)$. Then we use our trained ML model Θ_R to estimate the ripple noise penalty on the new connection $\Theta_R(f(r))$ and estimate the total noise including ripple as $G_{Noise\_REA} + \Theta_R(f(r))$. The testing error will be identified once we establish the connection, monitor the SNR and the noise at the receiver and compare it to that. The interactions between the collected monitoring information, the Qtool Q_{REA} and the ML assisted ripple noise penalty estimation are depicted in Fig. 8.
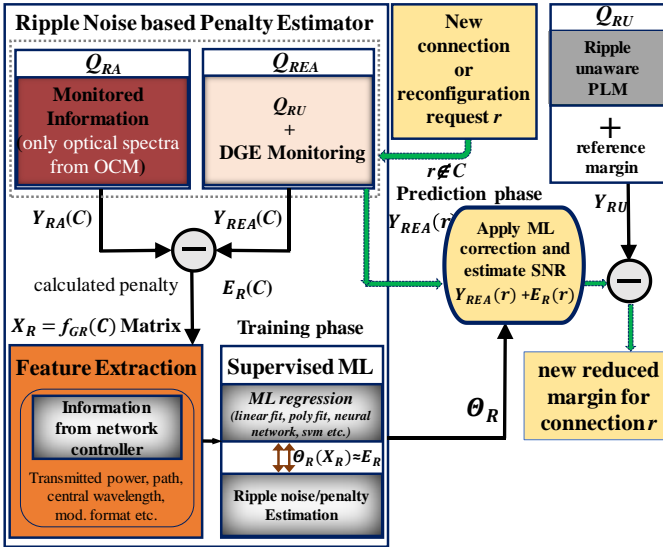

Fig 8. Overall flowchart of ML-based penalty estimator (i.e., train/test/estimate) for EDFA gain ripple case

B. ML-based node filter uncertainty modeling

The standard filter uncertainty unaware Qtool Q_{FU} starts from the transmitter parameters and calculates the cascaded attributes for identical filters down the path until the receiver. So, as discussed in Section IV.B, Q_{FU} implements the attribute dependent function w^j which calculates the attribute of the next link based on the attribute of the previous link, $s_{p_{c,m+1}}^j = w^j(s_{p_{c,m}}^j, F_m)$ for a specific filter F_m assuming no uncertainty $\Delta_{p_{c,m}}^j = 0$ (Fig. 6(a) shows a w^{3dB} function). Based on monitoring information we understand the actual filtering uncertainties and use that for estimation of future connections requests as described in the following.

We assume that OCMs are available at links ends to monitor the signal spectrum $S_{p_{c,m}}(p_c, \lambda_c)$ for all established connections c in C. As discussed in Section IV.B, from $S_{p_{c,m}}$ we can extract appropriate attributes $S_{p_{c,m}}^j$, which serve as the ground truth and are stored in Qtool database. Based on this OCM information $S_{p_{c,m}}^j$, we correct Q_{FU} as follows. We denote the expected

attributes from the monitored data of established connection C by $s_{p_{c,m+1}}^j = w^j(S_{p_{c,m}}^j, F_m)$. The monitored-expected error is given by $E_{p_{c,m+1}}^j = S_{p_{c,m+1}}^j - s_{p_{c,m+1}}^j$, which is due to unknown uncertainties $\Delta_{p_{c,m+1}}^j$. Then, we extract a per link ML features matrix, $X_{p_{c,m}}^j = f_{FA}(S_{p_{c,m}}^j, s_{p_{c,m}}^j)$. By concatenating all errors and features matrices for the different attributes j we obtain the overall error and the *filters attributes feature matrix*, E_F and X_F, respectively. Our goal is to identify a per link dependent (each link representing the WSS before and after it) error function Θ_F which maps the features matrix X_F to the error E_F, that is $\Theta_F(X_F) \approx E_F$. We rely on supervised ML regression techniques for training on E_F as target/label vector and finding Θ_F. Fig. 9 shows the features matrix X utilizing OCM data $S_{p_{c,m}}^j$, and the w^j expected attributes $s_{p_{c,m+1}}^j$ for the toy network of Fig.7.

Fig. 9. Link based generated filters attributes features matrix X_F for the sample network shown in Fig. 7 (4 nodes, with established connection from A to D).

Assuming a new connection request $r \notin C$, we start with its transmission spectrum parameters calculate the expected attributes for the next link using w^j, extract ML features (for known modulation format), use trained ML to predict the attributes correction (new E_F), apply that correction, and repeat that link by link down the path until destination. Then we translate the corrected expected filter attributes at the end of the path to the SNR penalty using function q, as discussed in Section IV.B (Fig. 6(b)). The pseudo-code of this process is given in Algorithm 1. The testing error will be identified once we establish the connection, measure SNR at the receiver and compare it to SNR estimated by Algorithm 1.

C. ML-based gain ripple and filter uncertainty modeling

In this case, when both effects are simultaneously present, we use all available monitors, OCM, DGE and Rx, together. We start by implementing the ML-based filter uncertainty model described in Section V.B. We use OCM monitored spectra, to obtain filter attributes, $S_{p_{c,m}}^j$. Then we use ripple and filter unaware Qtool, Q_{RFU} and its functions w^j to estimate the filtering attributes for next links and create filters attributes features matrix X_F (Fig. 9). We then train the ML model Θ_F. Then we use OSNR filter penalty estimation function q to calculate from the monitored attributes at end of the connections $S_{p_c}^j$ the related filter SNR penalties, denoted by $P_{FA}(C)$, which are assumed to be quite accurate since they come

Algorithm 1: link by link ML correction for testing dataset

1:	Input: New connection request $r \notin C$ Filters attributes feature matrix extraction f_{FA} Trained filter uncertainty ML model Θ_F
2:	Run RSA to assign wavelength λ_r, path p_r and other transmission parameters, e.g. filters BW Assume known filters shape F_m for all m in path p_r
3:	Assign Tx j-th attribute to $S^j_{p_{r,0}}$ and $s^j_{p_{r,0}}$
4:	**for** $m = 0: N-1$ (N is the number of links on path p_r)
5:	$s^j_{p_{r,m+1}} = w^j(S^j_{p_{r,m}}, F_m)$
6:	calculate $X^j_{p_{r,m}} = f_{FA}(S^j_{p_{r,m}}, s^j_{p_{r,m}})$
7:	use trained ML model to estimate the correction, $E^j_{p_{r,m+1}} = \Theta_F(X^j_{p_{r,m}})$
8:	apply correction, $s^j_{p_{r,m+1}} = s^j_{p_{r,m+1}} + E^j_{p_{r,m+1}}$
9:	**end** for
10:	Calculate SNR estimation error at receiver with q using corrected estimations at receiver $s^j_{p_r}$

from monitored data. We then used monitored SNR at the receivers (SNR_{RFA}) and subtract from those the filter penalties $P_{FA}(C)$ to obtain the SNR that includes only the gain ripple effect (SNR_{RA}). From that we obtain the accumulated noises $Y_{RA}(C)$ that include the ripple penalties. Then we use the DGE monitored data and the process described in Section V.A to create the ripple features matrix X_R and train the gain ripple ML model Θ_R. Note that this stepwise approach works because we have adequate monitoring information to distinguish between the two effects: OCMs gives us information to understand the filter penalty which we can then remove from the monitored SNR at the receivers and focus then on the gain ripple penalties. For new connection requests r, we follow the same order, and apply first the filter penalty correction based on Θ_F and then the ripple penalty correction Θ_R.

VI. RESULTS & DISCUSSION

To quantify the benefits of the developed accurate QoT estimators, we performed simulations to identify the amount of margin reduced in the presence of single or both gain ripple and filter penalty uncertainties. For this analysis, we consider Deutsche Telekom, DT topology with 12 nodes and 40 bidirectional links. The link lengths range from 48 to 458 km as shown in Fig. 10.

We assumed uncompensated bidirectional fiber links with spans of 80km of standard single-mode fiber (SSMF). We assumed 4 different traffic loads of {100, 200, 300, 400} total connections with uniformly chosen source-destination pairs. We served each demand with one wavelength, assumed to be modulated at 32Gbaud with a modulation-tunable pol-mux transponder. We assumed that the transponder could adapt to {QPSK, 8-QAM, 16-QAM} modulation formats, leading to {100, 150, 200} Gbps of datarate, respectively. We assumed a frequency slot size of 12.5GHz and allocated 3 spectrum slots for each 32Gbaud connection. We assumed a stable network *state*, where we have a specific set of connections established and we want to establish a new set of connections. As discussed

above, we exploit supervised machine learning to train the respective ML model on monitored connections to understand the gain ripple and filter uncertainty penalties. Then we use this trained ML model to estimate the 'unseen' penalties of the new connection requests with higher accuracy/lower design margin.
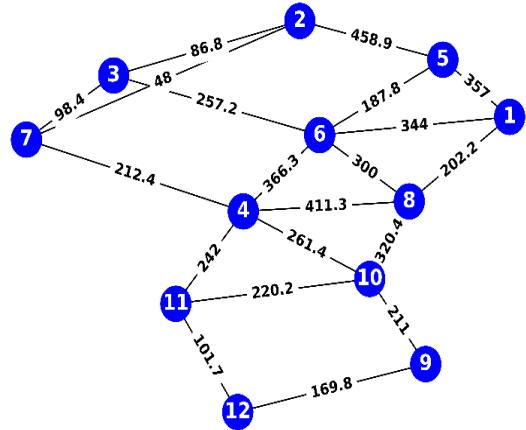

Fig. 10. DT 12 node network topology with length (in kms).

Assuming a specific set of connections, we routed them (with an RSA shortest path and first free slots algorithm) and then we generated monitored data using the *uncertainty aware* Qtools (Section IV and the Appendixes) with parameters described in the following paragraphs. We then divided the connections into two sets of 90%/10%, the training and testing datasets, respectively. The training set was assumed to be the established connections C and the testing set to correspond to the new connections to be established, $r \notin C$. We averaged the results over 200 iterations (random sources-destinations, and random split of training/testing data) at each load.

To study the effect of gain ripple we initially assumed no filtering uncertainty. We assigned experimentally measured gain ripple profiles, $g(\lambda)$, to each span EDFA, after applying random time shifting and amplitude scaling to them (see Section III). We assumed that OCM are installed before each ROADM node and that we can also monitor the power profiles applied by the DGEs through their feedbacks. All these were integrated in the ripple aware Qtool, Q_{RA}, that calculated the DGE power profiles and also the total noises at the receivers $Y_{RA}(C)$. Taking as reference the ripple unaware Qtool Q_{RU} (see Section IV.A and Appendix1), we depict in Fig. 11(a) the estimation error for 400 connections, which pertains to the ripple penalty. The penalties were distributed in positive and negative sides depending upon the ripple values and were ~1.8 dB in total. Positive/negative penalties result in upper/lower bounds for the design margin, which we call as "high/low margin". In standards ~2-3dB of design margin is typically used to accommodate all uncertainties [6]. Fig. 11(a) shows that ~1dB of QoT tool design margin would be required to accommodate the ripple penalties only (shown by histogram plot in dotted red circle). The remaining part of the design margin would cover the other uncertain effects. To improve the estimation accuracy, we used the ML model described in Section V.A. We used the DGE power profiles with the ripple-dynamic gain equalizer aware Q_{REA} Qtool to obtain the noise at the receiver, $Y_{REA}(C)$. By subtracting Y_{REA} and Y_{RA}, we obtain
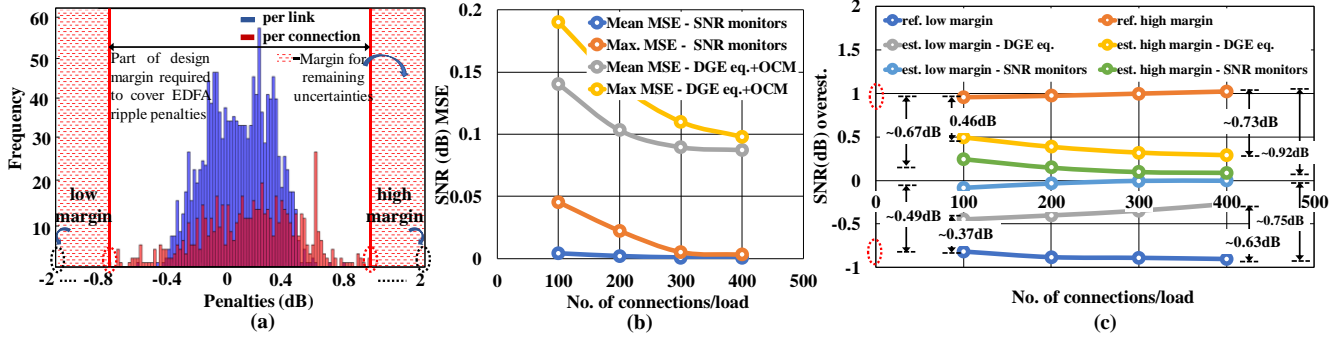
Fig. 11. Effect of ripple assuming no filtering uncertainty. (a) penalty distribution for 400 connections, indicating min. required design margin to accommodate ripple, (b) performance evaluation (MSE of SNR (dB)) of trained ML model on testing dataset, and (c) Max. overestimation error as a function of load.
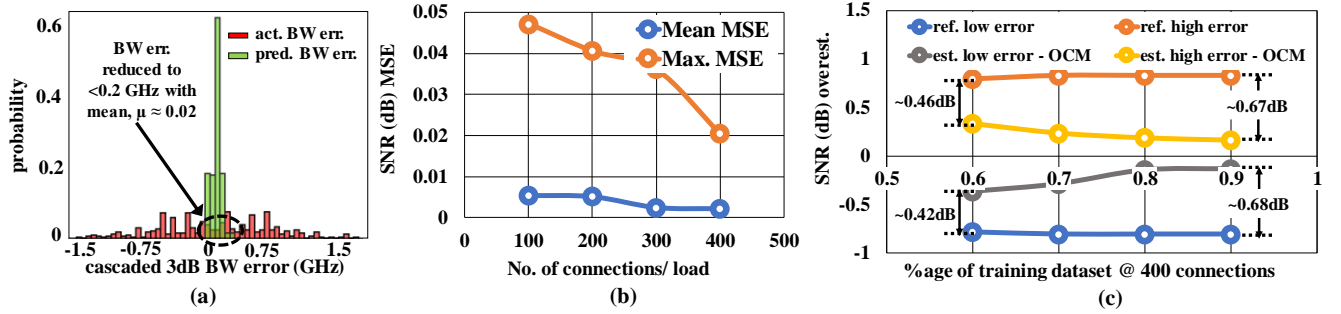

Fig. 12. Effect of filtering uncertainty assuming no gain ripples. (a) increase in 3dB BW prediction accuracy with ML along with error distribution (without ML), and (b) performance evaluation (MSE of SNR (dB)) of trained ML model on testing dataset, and (c) Max. overestimation error as a function of load.
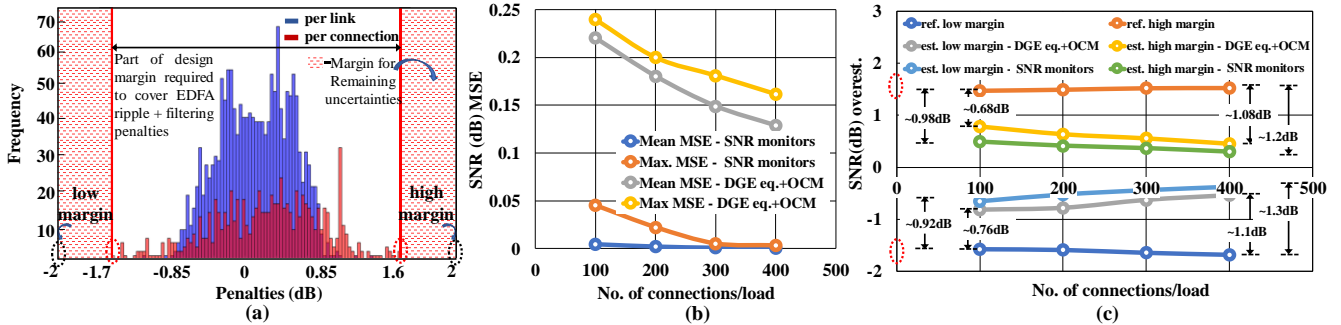

Fig. 13. Effects of both ripple with node uncertainties. (a) penalty distribution for 400 connections, indicating min. required design margin to accommodate ripple with node uncertainties, (b) performance evaluation (MSE of SNR (dB)) of trained ML model on testing dataset, and (c) Max. overestimation error as a function of load.

the penalty vector E_R. We then created the ripple feature matrix X_R and evaluated several ML assisted regression techniques to fit $\Theta_R(X_R)$ on E_R, such as linear fitting, quadratic, polynomial fitting, neural network, support vector machine regression (SVMR) etc. In the presented results we used SVMR with *linear* kernel function that achieved maximum Mean Squared Error (MSE) of ~0.19 on predicted SNR with load of 100 connections as shown in Fig. 11(b). In ML based regression models, MSE and root MSE (RMSE) are the key performance criteria to evaluate the estimation accuracy. By increasing the load from 100 to 400, the maximum MSE converges to a value of ~0.096. For the above set of simulations, the maximum used peak-to-peak ripple intensity among all span EDFAs was about ±0.5dB, which resulted in a reference margin ($design\ margin_1$) of ~1.02dB (max. of dotted red circle of histogram). Fig. 11(c) shows the maximum overestimation error on SNR, relative to Fig. 11(a). This overestimation is the reduced estimated high and low margin ($design\ margin_2$). For

high margin, it is found to be ~0.28dB, yielding a ~0.73dB margin reduction at a load of 400 connections. For low margin, we found ~0.63dB reduction as the distribution of penalties was less for low margin side. For comparison purposes we also plot in Fig. 11 (c) the results we obtained with our previous work [28]. In [28] we assume electrical SNR monitors available at each ROADM node, which is a quite strong assumption. With [28] we obtained a reduction of the high margin to 0.08dB, that is ~0.92dB improved accuracy. For low margin, we observed a reduction of ~0.75dB as shown in Fig. 11(c).

To study the effect of filter spectral shape uncertainties, we assumed flat EDFAs and we randomly applied small uncertainties Δ_m (resulted in end to end 3dB variation of ±1.5GHz) at each WSS. Such uncertainties would reflect Tx. and filters-grid mismatches, and small variations in filters shapes. We used the filter uncertainty aware Qtool, Q_{FA}, to calculate the ground truth, the 3dB BW of the connections on their paths, along with their SNR filter penalties. Then, for the

set of established connection C, we used the filter uncertainty unaware Qtool, Q_{FU}, to estimate the 3dB bandwidth and SNR filter penalties, and to calculate the errors with respect to the ground truth. Fig. 12(a) shows the distribution of the 3dB BW error at a load of 400 connections which has both positive and negative sides depending upon Δ_m. The corresponding SNR errors are also distributed in both polarities resulting in reference high and low margins. We then used the proposed ML based method discussed in Section V.B. We extracted the filters attributes features matrix, X_F and used the calculated attributes (only 3dB BW here) errors, E, to train a SVMR model (with *gaussian* kernel). Then for a new connection we used Algorithm 1, as described above, in a link by link estimation of 3dB BW down to the receiver. This was then used to estimate the filtering penalty which finally gives us the estimated SNR of the connection.

Fig. 12(a) shows the achieved error reduction in 3dB BW (from ±1.5GHz → ~0.18GHz) using the trained SVMR model. Fig. 12(b) shows a maximum MSE of ~0.04 dB on estimated SNR at a maximum load of 400 connections (200 times average @ 400 connections) using the trained SVMR model. Fig. 12(c) reflects the SNR accuracy / margin reduction as a function of the load. We observed a maximum error reduction/accuracy improvement of ~0.67dB for high margin and ~0.68dB for low margin, respectively. For high/low margin, we found an overall reduction of 80.4/83.4% at a load of 400 connections.

Then for the most realistic case of both effects present together in the network, we assigned ripple profiles (perturbating the experimentally collected profiles) at each EDFA and applied small 3dB BW uncertainties Δ_m^{3dB} at each WSS. Then we used the ripple and filtering uncertainties aware Qtool Q_{RFA} (see Section IV.C and Appendix3) to produce monitoring data. We obtained the SNR error distribution for 400 connections shown in Fig 13(a). Note that since we considered both effects, we ended up with wider error distribution than the individual cases discussed above.
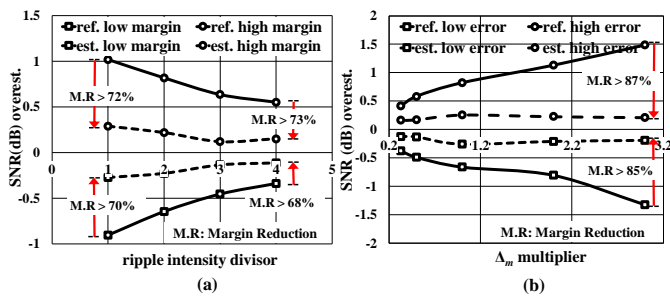

Fig. 14. New margins for (a) ripple and no node uncertainty, with different intensities of peak-to-peak gain ripple (reference as ±0.5dB), (b) filter and no ripple uncertainty, with reference $\Delta_m = \pm 10\%$.

To improve the estimation accuracy, we followed the process described in Section V.C to train the related ML models. We first accounted for the filtering penalties; using the monitored spectra we trained SVMR ML model θ_F. Then we removed the filtering penalties from the monitored SNR at the receivers to focus on the ripple. So, we trained θ_F to estimate the accumulated noise or ripple penalty. Figure 13(b) shows the obtained SNR MSE while (c) shows the reduction in the

reference high and lower margins. For high margin, the overall related margin savings is found to be ~1.2 dB and ~1.3 dB for the case of high and low margin, respectively.
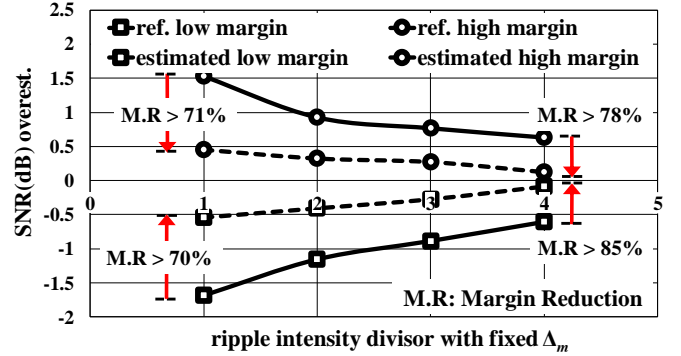

Fig 15. New reduced margin for different intensities of peak to peak gain ripple with fixed uncertainties, Δ_m inside ROADM node.

Finally, we extended our simulations to verify that the proposed ML based solution works for different intensities of ripple and filtering uncertainties and to quantify the related benefits. At first, we varied the gain ripple intensity, assuming only ripple with no filter uncertainty effect. We divided the span EDFA gain ripple profiles by a factor of 1 to 4, resulting in peak-to-peak fluctuations of ±0.5dB to ±0.125dB. We estimated the high and low margins at a fixed load of 400 connections as shown in Fig. 14(a). The obtained savings were higher than 70% for the examined peak-to-peak values. We then varied the filter attributes uncertainty Δ_m, assuming only filtering uncertainties. We multiplied Δ_m by a factor of 1/3 to 3 and estimated high and low margins/errors at a fixed load of 400 connections. Note that high value of Δ_m reflect ROADMs nodes with higher uncertainty, which are expected in disaggregated/ multi-vendor networks. As expected, higher reference margins are required in this scenario, and our accurate modeling results in more pronounced savings that reach >85% and >1.5 dB on both high and low margins.

Finally, when both uncertainties are present, we again varied peak-to-peak EDFA gain ripple intensity (similar to Fig. 14(a)) but this time we assumed a fixed range of node uncertainties ($\Delta_m = \pm 10\%$.). In Fig. 15 we show the reduction of the related margin at a load of 400 connections is achieved. For the examined intensities of the uncertainties, an overall margin reduction of >75% on both high and low margins.

VII. CONCLUSION AND FUTURE WORK

We proposed to use available monitored information from established connections and appropriate supervised ML to model the EDFA gain ripple and filtering penalties. We developed independent models for the two effects and then a joint model. The ML model would be then used for estimating the penalties of new connection requests, improving the Qtool estimation accuracy and thus reducing the required design margin. With combine span EDFA gain ripples and ROADM node uncertainties, we accomplished a design margin reduction of 1.68dB to 0.37dB for new connection requests with respect to the reference ripple and filtering uncertainty unaware Qtool.

In future, we plan to further verify the proposed approach on experimentally measured datasets. Also, we plan to integrate this intelligent Qtool with advanced resource allocation strategies, and quantify the reduction in overprovisioning and thus, the cost of future optical networks.

APPENDIX

Appendix1:

Assuming link m with N_s spans (Fig. 5), the PSD of ASE noise at the link end accumulated over span EDFAs is given by

$$G_{ase,m} = \sum_{n_s=1}^{N_s} NF_{n_s} * h * v * (g_{n_s} - 1) \qquad (2)$$

where, NF_{n_s} and g_{n_s} is the noise figure and average gain of n_s- th span EDFA, h is the Planks constant, v is the reference frequency (typically 193.1 THz).

Let us now assume that link m has N_{ch} WDM channels (Fig. 5). For channel n, we assume transmitted power P_n and symbol rate, R_n. In general, with incoherent noise accumulation assumption, the PSD of NLI noise at link end can be calculated as the sum of the NLI noise produced in each single span. With the assumption of noise to be additive gaussian, the GN model calculates PSD of NLI noise at link end, as

$$G_{nli,m}(\lambda_c) = \frac{16}{27} \sum_{n_s=1}^{N_s} \gamma_{n_s}^2 L_{eff,n_s}^2 \cdot$$

$$\sum_{n=1}^{N_{ch}} G_{n,n_s} G_{n,n_s} G_{c,n_s} (2 - \delta_{nc}) \Psi_{\lambda_n,\lambda_{n,n_s}} \cdot \qquad (3)$$

$$\prod_{n_s'=1}^{n_s-1} g_{n_s'}^3 e^{-6\alpha_{n_s'} L n_s'} \cdot \prod_{n_s'=n_s}^{N_s} g_{n_s'} e^{-2\alpha_{n_s'} L n_s'},$$

where Ψ is the phased array factor which under the assumption of incoherent accumulation is given by Eq. (128) and Eq. (129) of [46]; L_{n_s} is the n_s span length; γ_{n_s} is its non-linear coefficient; L_{eff,n_s} is its effective length; α_{n_s} is its attenuation coefficient, g_{n_s} is the gain of the span EDFA; $G_{n,ns}$ is the PSD of then n-th WDM channel (n=1, 2…, N_{ch}) at the start of the n_s-th span; δ_{nc} is the factor that distinguishes the SCI and XCI terms as given by Eq. (122) of [46]. The detailed derivation of Eq. (3) along with parameters description are available in [46]. A standard PLM/Qtool assumes that each fiber span loss ($e^{-2\alpha_{n_s} L_{n_s}}$) is *exactly* compensated at the end of each span by the gain of span EDFA (g_{n_s}). Also, a standard PLM assumes a flat/wavelength independent EDFA gain without ripple. Under this assumption the per span PSD of side channels ($G_{n,ns}$) and channel of interest at λ_c ($G_{c,ns}$), depends only on baud rate, R_n and per channel transmitted power, P_n. Thus, a standard PLM makes following assumptions on three terms of Eq. (3) as

$$\left\{ \begin{array}{c} \prod_{n_s'=1}^{n_s-1} g_{n_s'}^3 e^{-6\alpha_{n_s'} L n_s'} = 1 \\ \prod_{n_s'=n_s}^{N_s} g_{n_s'} e^{-2\alpha_{n_s'} L n_s'} = 1 \\ G_{n,n_s} = \frac{P_n}{R_n} \text{ for } n = 1, \dots N_{ch}, n_s = 1, \dots, N_s \end{array} \right\} \qquad (4)$$

The total NLI noise at channel centered at λ_c, $G_{nli,m}(\lambda_c)$ is calculated by using assumptions of Eq. (4) in Eq. (3) and is independent of per span wavelength dependent gain ripple effect. Also, the distortion introduced by a span EDFA ripple in

the PSD of the channels, which are input for the next span are not considered for the calculation of NLI noise of next span. We denote the PSD of NLI calculated with the ripple unaware equations, that is, Eq. (4) used in Eq. (3), as $G_{nli\_RU,m}(\lambda_c)$.

Assuming now a network and connection $c=(p_c, \lambda_c)$ crossing link m on its path p_c. The SNR at the end of link m calculated with the ripple unaware GN model, is given by

$$SNR_{RU,m}(p_c, \lambda_c) = \frac{G_{o,m}(\lambda_c)}{G_{ase,m} + G_{nli\_RU,m}(\lambda_c)} = \frac{G_{o,m}(\lambda_c)}{G_{Noise\_RU,m}(\lambda_c)} \qquad (5)$$

where $G_{o,m}(\lambda_c)$ is the output signal PSD at the end of link m which is equal to P_c/R_c for the assumptions of Eq. (4).

A typical assumption for a connection that traverses multiple links is that the inverse SNR per link is additive. With the ripple unaware PLM of Eq. (5) the total SNR at end of connection c is given by

$$[SNR_{RU}(p_c, \lambda_c)]_{dB} =$$

$$\left[1 \Big/ \left(\sum_{m \in p_c} SNR_{RU,m}^{-1}(p_c, \lambda_c) \right) \right]_{dB} + design\ margin_1 \qquad (6)$$

We now discuss how to extend the GN model to account for EDFA gain ripples. To model that, we assume known EDFA gain profiles for the span EDFAs, denoted by $g_{n_s}(\lambda)$ (for λ ranging the full C-band), which is broken down as follows

$$g_{n_s}(\lambda) = g_{n_s,avg} \cdot g_{n_s,r}(\lambda) \qquad (7)$$

where $g_{n_s,avg} = g_{n_s}$ (= span loss) is the average value and $g_{n_s,r}(\lambda)$ is the wavelength dependent ripple.

Each $g_{n_s,r}(\lambda)$ alters the current span signal PSD G_{n,n_s} of the next span depending. This clearly means that to accommodate the ripple effect in $G_{nli}(\lambda_c)$ calculations, the assumptions in Eq. (4) need modifications and extensions at span level as follows:

$$\left\{ \begin{array}{c} \prod_{n_s'=1}^{n_s-1} [g_{n_s',avg} \cdot g_{n_s',r}(\lambda_c)]_{n_s'}^3 e^{-6\alpha_{n_s'} L n_s'} \neq 1 \\ \prod_{n_s'=n_s}^{N_s} [g_{n_s',avg} \cdot g_{n_s',r}(\lambda_c)]_{n_s'} e^{-2\alpha_{n_s'} L n_s'} \neq 1 \\ G_{n,n_s} = \left(\begin{array}{c} \frac{P_n}{R_n}; n_s = 1 \\ \sum_{n_s'=1}^{n_s-1} G_{n,n_s'} \cdot g_{n_s',r}(\lambda_n); n_s \neq 1 \end{array} \right), n = 1, \dots N_{ch} \end{array} \right\}$$

(8)

This Eq. (8) is then substituted in Eq. (3) to calculate the ripple aware NLI noise $G_{nli\_RA,m}(\lambda_c)$ that takes into account *per span* wavelength dependent ripple effects in gain as well as the PSD of the lighted channels. Also, DGE altered power profile (from mid span) modifies the NLI noise contribution for all onward spans. We can capture this with Eq. (8) by setting the DGE applied channels PSD $G_{n,n_{DGE}}$ at the specific span n_{DGE}. Using the extended GN model, we obtain the SNR calculated at the end of link m, $G_{nli\_RA,m}(\lambda_c)$. So, Eq. (5), is now changed to Eq. (9) as

$$SNR_{RA,m}(p_c, \lambda_c) = \frac{G_{o,m}(\lambda_c)}{G_{ase,m} + G_{nli\_RA,m}(\lambda_c)} =$$

$$\frac{G_{o,m}(\lambda_c)}{G_{ase,m} + G_{nli\_RU,m}(\lambda_c) + G_{RA,m}(\lambda_c)} = \frac{G_{o,m}(\lambda_c)}{G_{Noise\_RA,m}(\lambda_c)} \qquad (9)$$

where $G_{Noise\_RA,m}(\lambda_c)$ corresponds to the total noise at the end of link m estimated by the PLM with EDFA gain ripple information. With this PLM, plus an additional margin, the total

SNR calculated at end of connection $c=(p_c, \lambda_c)$ traversing L links is given by

$$[SNR_{RA}(p_c, \lambda_c)]_{dB} =$$

$$\left[1 / \left(\sum_{m \in p_c} SNR_{RA,m}^{-1}(p_c, \lambda_c) \right) \right]_{dB} + design\ margin_2 \quad (10)$$

Appendix 2:

The filtering penalty assuming identical filters is based on some predefined function/measurement (such as in Fig. 6) and is unaware of the uncertainties due to the spectral variations of the filters ($\Delta_m^j = 0$). This results in filter uncertainty unaware penalty denoted by G_{FU}. This G_{FU} results in the following SNR over subpath $p_{c,m}$, at the end of the link m and before the next node:

$$SNR_{RU,m}(p_c, \lambda_c) = \left(\frac{G_{o,m}(\lambda_c)}{G_{ase,m} + G_{nli\_RU,m}(\lambda_c)} \right). G_{FU}(p_{c,m}) \quad (11)$$

In a real network, $\Delta_m^j \neq 0$ results in a different filtering uncertainty aware penalty, G_{FA}, AND hence inaccurate QoT estimation. Assuming known Δ_m^j for all filters, and thus known subpath penalties $G_{FA}(p_{c,m})$ the SNR at the end of the link m before the next node is given by

$$SNR_{FA,m}(p_c, \lambda_c) = \left(\frac{G_{o,m}(\lambda_c)}{G_{ase,m} + G_{nli\_RA,m}(\lambda_c)} \right). G_{FA}(p_{c,m}) \quad (12)$$

To calculate the SNR at the end of connection c with multiple links i.e. $SNR_{FU}(p_c, \lambda_c)$ and $SNR_{FA}(p_c, \lambda_c)$, we extend Eq.(11) and Eq.(12) using the inverse SNR linear additive assumption (similar to Eq.(6) and Eq.(10)).

Appendix 3:

For connection, c, the filter penalty generated by identical filters for subpath $p_{c,m}$ is $G_{FU}(p_{c,m})$ and the PSD of NLI noise by flat ripple EDFsA is $G_{RU}(\lambda_c)$. The overall accumulated noise, G_{Noise_RFU} and the equivalent SNR calculated at link m end is given by

$$SNR_{RFU,m}(p_c, \lambda_c) = \left(\frac{G_{o,m}(\lambda_c)}{G_{Noise\_RFU}(\lambda_c)} \right). G_{FU}(p_{c,m}) \quad (13)$$

where

$$G_{Noise\_RFU,m}(\lambda_c) = G_{ase,m} + G_{nli\_RU,m}(\lambda_c)$$

Similarly, the penalty generated with known non-identical filter responses, $\Delta_i^j \neq 0$ for subpath $p_{c,m}$ is $G_{FA}(p_{c,m})$ and the PSD of NLI noise generated by EDFAs with known gain ripples, is $G_{nli\_RA}(\lambda_c)$. The overall accumulated noise, $G_{Noise\_RFA,m}$ and SNR calculated at the end of link m is given by

$$SNR_{RFA,m}(p_c, \lambda_c) = \left(\frac{G_{o,m}(\lambda_c)}{G_{Noise\_RFA,m}(\lambda_c)} \right). G_{FA}(p_{c,m}) \quad (14)$$

where

$$G_{Noise\_RFA,m}(\lambda_c) = G_{ase,m} + G_{nli\_RA,m}(\lambda_c) + G_{RA,m}(\lambda_c)$$

To calculate the SNR at the end of connection c with multiple links i.e. $SNR_{RFU}(p_c, \lambda_c)$ and $SNR_{RFA}(p_c, \lambda_c)$, we extend Eq.(13) and Eq.(14) using the inverse SNR linear additive assumption (similar to Eq.(6) and Eq.(10)).

REFERENCES

[1] V. Lopez and L. Velasco (Editors), "Elastic Optical Networks. Architectures, Technologies, and Control," Springer, 2016.

[2] P. Lu, L. Zhang, X. Liu, J. Yao, and Z. Zhu, "Highly efficient data migration and backup for big data applications in elastic optical inter-data-center networks," IEEE Netw., vol. 29, pp. 36-42, 2015.

[3] O. Gerstel, M. Jinno, A. Lord, and S. J. B. Yoo, "Elastic optical networking: a new dawn for the optical layer?," IEEE Commun. Mag., vol. 50, pp. S12-S20, Apr. 2012

[4] K. Roberts, Q. Zhuge, I. Monga, S. Gareau, and C. Laperle, "Beyond 100 Gb/s: capacity, flexibility, and network optimization [Invited]," J. Opt. Commun. Netw., vol. 9, no. 4, pp. C12-S23, Apr. 2017.

[5] A. Mitra, A. Lord, S. Kar, and P. Wright, "Effect of link margin and frequency granularity on the performance of a flexgrid optical network," Opt. Express, vol. 22, no. 1, pp. 41-46, Jan. 2014.

[6] Y. Pointurier, "Design of Low-Margin Optical Networks," J. Opt. Commun. Netw., vol. 9, no. 1, pp. A9-A17, Jan. 2017.

[7] J. L. Auge, "Can we use Flexible Transponders to Reduce Margins? ," in Proc. of OFC, 2013.

[8] E. Seve, J. Pesic, C. Delezoide, S. Bigo, and Y. Pointurier, "Learning Process for Reducing Uncertainties on Network Parameters and Design Margins," J. Opt. Commun. Netw., vol. 10, no. 2, pp. A298-A306, Feb. 2018.

[9] I. Sartzetakis, K. Christodoulopoulos, C. P. Tsekrekos, D. Syvridis, E. Varvarigos, "Quality of transmission estimation in WDM and elastic optical networks accounting for space–spectrum dependencies," J. Opt. Commun. Netw., vol. 8, no. 9, pp. 676-688, Sep. 2016.

[10] L. Barletta, A. Giusti, C. Rottondi, and M. Tornatore, "QoT estimation for unestablished lighpaths using machine learning," in Proc. of OFC, 2017.

[11] I. Sartzetakis, K. Christodoulopoulos, and E. Varvarigos, "Accurate quality of transmission estimation with machine learning," J. Opt. Commun. Netw., vol. 11, no. 3, pp. 140-150, Mar. 2019.

[12] B. Pedersen, A. Bjarklev, J. H. Povlsen, K. Dybdal, and C. C. Larsen, "The design of erbium-doped fiber amplifiers," J. Lightw. Technol., vol. 9, no. 9, pp. 1105-1112, Sep. 1991.

[13] J. Zyskind, and A. Srivastava, "Optically Amplified WDM Networks: Principles and Practices," Elsevier, 2011.

[14] K. Ishii, J. Kurumida, S. Namiki, "Wavelength Assignment Dependency of AGC EDFA Gain Offset under Dynamic Optical Circuit Switching Learning," in Proc. of OFC, 2014.

[15] https://www.cisco.com/c/en/us/td/docs/optical/15000r7_0/dwdm/planning/guide/70epg/d7ina.html

[16] R. Peretti, B. Jacquier, D. Boivin, E. Burov, and A. M. Jurdyc, "Inhomogeneous gain saturation in EDF: Experiment and modeling," J. Lightw. Technol., vol. 29, no. 10, pp. 1445–1452, May 2011.

[17] L. Qiao, A. Solheim, Q. Bu, Y. Luo, C. Fu, W. Zhang, and M. Le, "Erbium Doped Fiber Amplifier with Passive Temperature Compensation," in Proc. of OFC, 2017.

[18] W. J. Miniscalco and R. S. Quimby, "General procedure for the analysis of Er^3+ cross sections," Opt. Letters, vol. 16, no. 4, pp. 258-260, Feb. 1991

[19] T. A. Strasser, and J. L. Wagener, "Wavelength-selective switches for ROADM applications," J. Sel. Areas Quan. Elec., vol. 16, no. 5, pp. 1150–1157, Oct. 2010.

[20] F. Paolucci, F. Cugini, F. Fresi, G. Meloni, A. Giorgetti, N. Sambo, L. Potí, A. Castro, L. Velasco, and P. Castoldi, "Superfilter technique in SDN-controlled elastic optical networks [Invited]," J. Opt. Commun. Netw., vol. 7, no. 2, pp. A285-A292, Dec. 2014.

[21] B. Collings, "New devices enabling software-defined optical networks," Commun. Maga., vol. 51, no. 3, pp. 66–71, Mar. 2013.

[22] J. M. Fabrega, M. S. Moreolo, L. Martín, A. C. Piat, E. Riccardi, D. Roccato, N. Sambo, F. Cugini, L. Potì, S. Yan, E. Hugues-Salas, D. Simeonidou, M. Gunkel, R. Palmer, S. Fedderwitz, D. Rafique, T. Rahman, H. Waardt, and A. Napoli, "On the filter narrowing issues in

elastic optical networks," J. Opt. Commun. Netw., vol. 8, no. 7, pp. A23–A33, Jul. 2016.

[23] T. Rahman, A. Napoli, D. Rafique, B. Spinnler, M. Kuschnerov, I. Lobato, B. Clouet, M. Bohn, C. Okonkwo, and H. Waardt, "On the Mitigation of Optical Filtering Penalties Originating from ROADM Cascade," Phot. Technol. Lett., vol. 26, no. 2, pp. 154–157, Jan. 2014.

[24] C. Delezoide, et al., "Automated Alignment Between Channel and Filter Cascade," OFC, 2019

[25] L. Velasco, A. Sgambelluri, R. Casellas, L. Gifre, J. L. I. Zaragoza, F. Fresi, F. Paolucci, R. Martínez, E. Riccardi, "Building autonomic optical white box-based networks," J. Lightw. Technol., vol. 36, no. 15, pp. 3097–3104, Aug 2018.

[26] M. Filer, M. Cantono, A. Ferrari, G. Grammel, G. Galimberti, and V. Curri, "Multi-vendor experimental validation of an open source QoT estimator for optical networks," J. Lightw. Technol., vol. 36, no. 15, pp. 3073–3082, Aug. 2018.

[27] K. Christodoulopoulos, C. Delezoide, N. Sambo, A. Kretsis, I. Sartzetakis, A. Sgambelluri, N. Argyris, G. Kanakis, P. Giardina, G. Bernini, D. Roccato, A. Percelsi, R. Morro, H. Avramopoulos, P. Castoldi, P. Layecet and S. Bigo, "Toward efficient, reliable, and autonomous optical networks: the ORCHESTRA solution [Invited]," J. Opt. Commun. Netw., vol. 11, no. 9, pp. C10–C24, Sep. 2019.

[28] A. Mahajan, K. Christodoulopoulos, R. Martínez, S. Spadaro and R. Muñoz, "Machine Learning Assisted EDFA Gain Ripple Modelling for Accurate QoT Estimation," in Proc. of ECOC, 2019.

[29] R. Munoz, R. Casellas, R. Martınez, and R. Vilalta, "PCE: What is It, How Does It Work and What are Its Limitations?," J. Lightw. Technol., vol. 32, no. 4, pp. 528–543, Aug 2018.

[30] M. Menif, L. A. Rusch, and M. Karasek, "Application of pre-emphasis to achieve flat output OSNR in time-varying channels in cascaded EDFAs without equalization," J. Lightw. Technol., vol. 19, no. 10, pp. 1440–1452, Oct. 2001.

[31] S. J. Savory, R. J. Vincent and D. J. Ives, "Design considerations for low-margin elastic optical networks in the nonlinear regime [Invited]," J. Opt. Commun. Netw., vol. 11, no. 10, pp. C76-C85, Oct. 2019.

[32] Y. Huang, C. L. Gutterman, P. Samadi, P. B. Cho, W. Samoud, C. Ware, M. Lourdiane, G. Zussman, And K. Bergman, "Dynamic mitigation of EDFA power excursions with machine learning," Opt. Express, vol. 25, no. 3, pp. 2245–2258, 2017.

[33] S. Zhu, C. L. Gutterman, W. Mo, Y. Li, G. Zussman, and D. C. Kilper, "Machine Learning Based Prediction of Erbium-Doped Fiber WDM Line Amplifier Gain Spectra," in Proc. of ECOC, Sep. 2018.

[34] S. Zhu, C. Gutterman, A. D. Montiel, J. Yu, M. Ruffini, G. Zussman, and D. Kilper, "Hybrid Machine Learning EDFA Model," in Proc. of OFC, 2020.

[35] Y. You, Z. Jiang, and C. Janz, "Machine learning-based EDFA gain model," in Proc. of ECOC, Sep. 2018.

[36] W. Mo, C. L. Gutterman, Y. Li, S. Zhu, G. Zussman, and D. C. Kilper, "Deep-neural-network-based wavelength selection and switching in ROADM systems," J. Opt. Commun. Netw., vol. 10, no. 10, pp. D1-D11, Oct. 2018.

[37] S. Zhu, C. Gutterman, A. D. Montiel, J. Yu, M. Ruffini, G. Zussman, and D. Kilper, "Neural Network Based Wavelength Assignment in Optical Switching," in Proc. of the Workshop on Big Data Analytics and Machine Learning for Data Communication Networks, 2017.

[38] C. Delezoide, P. Ramantanis, and P. Layec, "Weighted Filter Penalty Prediction for QoT Estimation," in Proc. of OFC, 2018.

[39] J. Pan and S. Tibuleac, "Real-Time ROADM Filtering Penalty Characterization and Generalized Precompensation for Flexible Grid Networks," IEEE Photonics Journal, vol. 9, no. 3, Jun. 2017.

[40] M.P. Belanger, M. O'Sullivan and P. Littlewood, "Margin requirement of disaggregating the DWDM transport system and its consequence on application economics," in Proc. of OFC, 2018.

[41] https://www.finisar.com/roadms-wavelength-management/foa-m7100da-evg2c-aa0xx

[42] https://www.nistica.com/fullfledge.html

[43] A. Bononi, P. Serena, N. Rossi, E. Grellier, and F. Vacondio, "Modeling nonlinearity in coherent transmissions with dominant intrachannel four-wave-mixing," Opt. Express, vol. 20, no. 7, pp. 7777–7791, Mar. 2012.

[44] P. Poggiolini, G. Bosco, A. Carena, V. Curri, Y. Jiang, and F. Forghieri, "The GN-model of fiber non-linear propagation and its applications," J. Lightw. Technol., vol. 32, no. 4, pp. 694–721, Feb. 2014.

[45] R. Dar, M. Feder, A. Mecozzi, and M. Shtaif, "Properties of nonlinear noise in long, dispersion-uncompensated fiber links," Opt. Express, vol. 21, no. 22, pp. 25685–25699, 2013.

[46] P. Poggiolini, G. Bosco, A. Carena, V. Curri, Y. Jiang, and F. Forghieri, "A detailed analytical derivation of the GN model of non-linear interference in coherent optical transmission systems," arXiv:1209.0394, 2014.

[47] https://www.finisar.com/roadms-wavelength-management/focm01fxc1mn